Transparent Micrometer-Thick TiO_2 Films on SiO_2-Coated Glass Prepared by Repeated Dip-Coating/Calcination: Characteristics and Photocatalytic Activities for Removing Acetaldehyde or Toluene in Air

Nobuaki Negishi,*[,†,‡] Sadao Matsuzawa,[†] Koji Takeuchi,[†] and Pierre Pichat[‡]

Research Institute for Environmental Management Technology, National Institute of Advanced Industrial Science and Technology (AIST), 16-1 Onogawa, Tsukuba 305-8569, Japan, and Photocatalyse et Environment, Centre National de la Recherche Scientifique (CNRS)/Ecole de Centrale de Lyon, 69134 Ecully, France

Received February 2, 2007. Revised Manuscript Received May 24, 2007

TiO_2 films on silica-coated glass plates were obtained through dip-coating and subsequent calcination at 753 K; this temperature and the proportions of the dip-coating solution components (tetraisopropyl orthotitanate, ethoxyethoxyethanol, propan-2-ol, α-terpineol, and a hydroxypropyl cellulose) were optimized. Depending on the number N ($5 \leq N \leq 30$) of dip-coating/calcination procedures, the films characteristics were hardness, >9 H; thickness, 0.9−5.4 μm; transmitted light, ca. 70% (visible spectral region); absorbed light, 90−100% at 358 nm; surface area, 40−80 $m^2\ g^{-1}$; pore volume 7−20 mL g^{-1}; anatase particle size, 3.5−4 nm (elemental crystallites) and 12−16 nm (agglomerates). These tiny sizes, which did not increase for $N \geq 20$, were obtained because of the use of hydroxypropyl cellulose. The photocatalytic removal rate of acetaldehyde (3.25 ppmv) or toluene (1 ppmv) in flowing air (50% RH) showed that the TiO_2 minimum amount varied with the pollutant and that a 1−2 μm thickness was sufficient to achieve a near-maximum efficacy. In summary, this preparation produces anatase films having the mechanical, optical, and photocatalytic properties required to obtain self-cleaning (water contact angle test) and air depolluting (at least in relatively confined spaces) glass without using a binder, which can restrict the accessibility to TiO_2 and alter the photocatalytic activity.

Introduction

Self-cleaning glass based on TiO_2 photocatalysis must be transparent (at least for most uses), highly durable, and of course sufficiently efficient for the elimination of visible deposits, which is its purpose.[1−12] This latter property, which is opposite to the other two, is generally fulfilled by <100 nm thick coatings as slow kinetics are acceptable, even though an efficacy as high as possible is obviously desirable. Seeking a higher photocatalytic efficacy is of interest not only to improve desoiling but also to take advantage of the potentiality of TiO_2-coated glass covering buildings to contribute to urban air purification, at least in relatively confined spaces such as canyon streets.[13,14] A higher photocatalytic efficacy can be obtained by increasing the TiO_2 surface area and the coating thickness and porosity to increase the adsorption of air pollutants.[15−17] However, thicker layers can have a lower transparency and be less solidly affixed to the glass support. Better anchored TiO_2 films on silica (or silica-containing) supports can be produced by (i) using an inorganic binder such as colloidal silica (or silica organic precursors),[18,19] (ii) calcinating the coated TiO_2 gel,[20−25] or (iii) using a SiO_2−TiO_2 binary system.[11,26−28]

* Corresponding author. Tel: 81-29-861-8165. Fax: 81-29-861-8866. E-mail: n-negishi@aist.go.jp.

† National Institute of Advanced Industrial Science and Technology (AIST).

‡ Centre National de la Recherche Scientifique (CNRS)/Ecole de Centrale de Lyon.

(1) Heller, A. *Acc. Chem. Res*. **1995**, *28*, 503.
(2) Paz, Y.; Luo, Z.; Rabenberg, L.; Heller, A. *J. Mater. Res*. **1995**, *10*, 2842.
(3) Sitkiewitz, S.; Heller, A. *New J. Chem*. **1996**, *20*, 233.
(4) Romeas, V.; Pichat, P.; Guillard, C.; Chopin, T.; Lehaut, C. *New J. Chem*. **1999**, *23*, 365.
(5) Romeas, V.; Pichat, P.; Guillard, C.; Chopin, T.; Lehaut, C. *Ind. Eng. Chem. Res*. **1999**, *38*, 3878.
(6) Tryk, D. A.; Fujishima, A.; Honda, K. *Electrochim. Acta* **2000**, *45*, 2363.
(7) Puzenat, E.; Pichat, P. *J. Photochem. Photobiol., A* **2003**, *160*, 127.
(8) Mills, A.; Lepre, A.; Elliott, N.; Bhopal, S.; Parkin, I. P.; O'Neill, S. A. *J. Photochem. Photobiol., A* **2003**, *160*, 213.
(9) Guan, K. *Surf. Coat. Technol*. **2005**, *191*, 155.
(10) Parkin, I. P.; Palgrave, R. G. *J. Mater. Chem*. **2005**, *15*, 1689.
(11) Zhang, X.; Sato, O.; Taguchi, M.; Einaga, Y.; Murakami, T.; Fujishima, A. *Chem. Mater*. **2005**, *17*, 696.
(12) Watanabe, T.; Nakajima, A.; Wang, R.; Minabe, M.; Koizumi, S.; Fujishima, A.; Hashimoto, K. *Thin Solid Films* **1999**, *351*, 260.
(13) Takeuchi, K.; Negishi, N.; Kutsuna, S.; Ibusuki, T. In *Proceedings of Materials Solutions for Environmental Problems*; Mostaghaci, H., Ed.; Canadian Institute of Mining, Metallurgy and Petroleum: Ottawa, Canada, 1997; p 162.
(14) Takeuchi, K. *Sci. Avenir* **2001**, 70.
(15) Negishi, N.; Takeuchi, K.; Ibusuki, T. *J. Mater. Sci*. **1998**, *33*, 5789.
(16) Yu, J.; Zhao, X.; Zhao, Q. *Mater. Chem. Phys*. **2001**, *69*, 25.
(17) Kominami, H.; Kumamoto, H.; Kera, Y.; Ohtani, B. *Appl. Catal., B* **2001**, *30*, 329.
(18) Avila, P.; Bahamonde, A.; Blanco, J.; Sánchez, B.; Cardona, A. I.; Romero, M. *Appl. Catal., B* **1998**, *17*, 75.
(19) Minabe, T.; Tryk, D. A.; Sawunyama, P.; Kikuchi, Y.; Hashimoto, K.; Fujishima, A. *J. Photochem. Photobiol., A* **2000**, *137*, 53.
(20) Negishi, N.; Iyoda, T.; Hashimoto, K.; Fujishima, A. *Chem. Lett*. **1995**, 841
(21) Kato, K.; Tsuzuki, A.; Torii, Y.; Taoda, H.; Kato, T.; Butsugan, Y. *J. Mater. Sci*. **1995**, *30*, 837.
(22) Yoko, T.; Hu, L.; Kozuka, H.; Sakka, S. *Thin Solid Films* **1996**, *283*, 188.

10.1021/cm070320i CCC: $37.00
Published on Web 06/29/2007

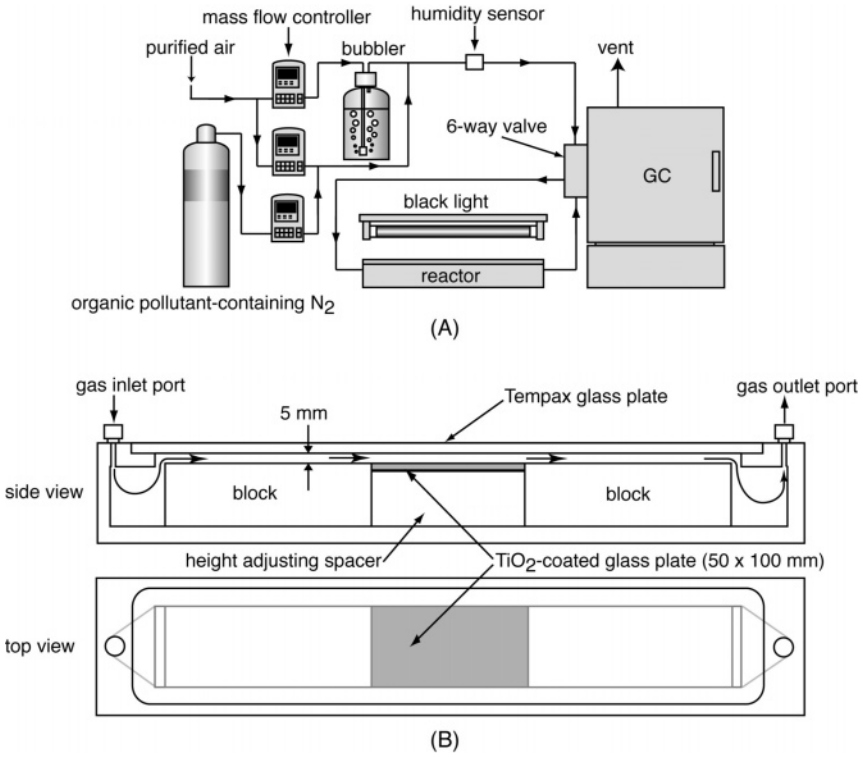

Figure 1. Schemes showing the device (A) and the reactor (B) used for measuring the photocatalytic activities.

Unfortunately, silica can partially embed the TiO_2 particles as was shown, for instance, for a coating on glass fiber,[29] and calcination can reduce their size, which results in a decrease in the photocatalytically active accessible surface area.

Consequently, in our dip-coating/calcination procedure, a silica binder was not utilized, and the aim of calcination was not only to affix the coating but also to produce TiO_2 from the gel directly on the support and not in the dip-coating solution.[30] To that end, water was excluded to avoid hydrolysis of the Ti alkoxide before calcination. This methodology had the advantage of allowing one to repeat the dip-coating/calcination procedure many times with the same dip-coating solution. Two other parts of our strategy to prepare thick TiO_2 films with high surface area and porosity included the use of (i) a highly viscous solvent (α-terpineol) to increase the film thickness at the surface of the glass plate during dip-coating,[30−32] and (ii) a component (hydroxypropyl cellulose) that, by being linked to the Ti alkoxide, prevented the TiO_2 particles from growing too fast and coalescing.[33,34] For TiO_2 films prepared with different numbers (N) of dip-coating/calcination procedures, we report here (i) several optical, structural, textural, and mechanical characteristics, and (ii) photocatalytic activities measured in a flow-type reactor for the removal in air of low concentrations of acetaldehyde or toluene as representative volatile organic compounds (VOCs).

2. Experimental Section

Preparation of TiO_2 Films. The solution for dip-coating was composed of tetraisopropyl orthotitanate (TPOT; Wako Chemical Co., 100 mL) as a TiO_2 source, ethoxyethoxyethanol (EEE; Wako Chemical Co., 100 mL) as a ligand for TPOT, propan-2-ol (2-PrOH; Wako Chemical Co., 150 mL) as solvent, and α-terpineol (TPO; Tokyo Kasei Co., 350 mL) as an additional highly viscous solvent. In addition, a hydroxypropyl cellulose 80000 (HPC; Wako Chemical Co., 6.25×10^{-4} mol/L)/2-PrOH solution (100 mL) was added to the above dip-coating solution under thorough mixing.

The viscosity of the dip-coating solution was measured with a Brookfield DV−I$^+$. An Otsuka ELS-8000 laser particle size analyzer was used to observe the particles in the solution. A TiO_2 gel for thermal analysis was obtained on drying 1 mL of the coating solution. The thermal analysis of this TiO_2 gel was carried out using a Shimadzu TG/DTA50 thermal analyzer between room temperature and 1033 K under flowing air (20 mL/min) in order to choose the most appropriate calcination temperature.

Preparation and Characterization of the TiO_2 Films. For preparing the TiO_2 films, the dip-coating method was applied. We used silica-coated glass plates (100 × 150 × 1.1 mm) as support. The withdrawing speed of the glass plate from the dip-coating solution was 1.5 mm/min. The dip-coated glass plates were treated at 753 K for 1 h. Five thicknesses of TiO_2 films were obtained by

(23) Sunada, K.; Kikuchi, Y.; Hashimoto, K.; Fujishima, A. *Environ. Sci. Technol*. **1998**, *32*, 726.
(24) Negishi, N.; Takeuchi, K.; Ibusuki, T.; Datye, A. K. *J. Mater. Sci. Lett*. **1999**, *18*, 515.
(25) Negishi, N.; Takeuchi, K. *Mater. Lett*. **1999**, *38*, 150.
(26) Yan, Y.; Chaudhuri, S. R.; Sarkar, A. *J. Am. Ceram. Soc*. **1996**, *79*, 1061.
(27) Renous-Chan, V. WIPO Patent WO-97/10186, 1997.
(28) Kwon, C.; Kim, J.; Jung, I.; Shin, H.; Yoon, K. *Ceram. Int.* **2003**, *29*, 851.
(29) Enriquez, R.; Beaugiraud, B.; Pichat, P. *Water Sci. Technol*. **2004**, *49*, 147.
(30) Negishi, N.; Takeuchi, K. *Thin Solid Films* **2001**, *392*, 249.
(31) Smirnova, N.; Eremenko, A.; Gayvoronskij, V.; Petrik, I.; Gnatyuk, Y.; Krylova, G.; Korchev, A.; Chuiko, A. *J. Sol−Gel Sci. Technol.* **2004**, *32*, 357.
(32) Liu, X.; Jin, Z.; Bu, S.; Yin, T. *J. Sol−Gel Sci. Technol.* **2005**, *36*, 103.
(33) Lee, D. S.; Liu, T. K. *J. Sol−Gel Sci. Technol.* **2002**, *25*, 121.
(34) Negishi, N.; Takeuchi, K. *Res. Chem. Intermed*. **2003**, *29*, 861.

varying the number N (5, 10, 15, 20, and 30) of dip-coating and sintering procedures.

For each film, the transmittance spectrum was measured using a Shimadzu UV-3600 UV−vis double-beam spectrometer. A Mamiya OP-QuoreMSPA1000 optical analyzer was used to measure the film thickness. The contact angle on each film was determined according to the standard test method JIS R3257 with a DropMaster 300 contact angle detector (Kyowa Interface Science Co.), and the measurements were carried out both under room light and after UV irradiation for 2 h (λ_{max} = 365 nm, 1 mW/cm^2). The cross section of the film was observed with a Hitachi SEM-4700 field emission scanning electron microscope (FE-SEM). The surface texture of the film was observed by atomic force microscopy (AFM; Shimadzu SPM-9300J apparatus). The film crystal structure was identified using a Rotaflex RU-300 (Cu Kα radiation at 40 kV and 80 mA) X-ray diffraction spectrometer (XRD). A Quantachrome AS-1 surface analyzer with N_2 adsorption was employed to measure surface areas and pore size distributions. The film hardness was determined according to the standard test method JIS K5600-5-4 (identical to ISO/DIS 15184) with an Imoto IMC-1552 pencil scratch hardness tester.

Measurement of the Photocatalytic Activity of the TiO_2 Films in the Gas Phase. The photocatalytic activity of the five TiO_2 films was measured from the elimination rate of 3 ppmv acetaldehyde or 1 ppmv toluene in air using the device shown in Figure 1. Dry air was mixed with water saturated air (Figure 1A) to obtain a RH of 50%, taking into account a low flow rate of dry N_2 containing the organic pollutant and a controlled temperature of 297 K. The RH was checked with a humidity sensor (CHINO MR6661). The size of the TiO_2-coated plate placed into the photocatalytic reactor was 100 × 50 × 1.1 mm (Figure 1B). A 10 W black light lamp (λ_{max} = 358 nm) was used; the irradiance at the surface of the photocatalyst was adjusted to 1 mW/cm^2, i.e., on the same order of magnitude as the solar irradiance on a horizontal plane in the UV-A spectral region. Each sample was pretreated under UV-irradiation for 16 h in order to clean the photocatalyst surface. Air contaminated with either acetaldehyde or toluene was then flowed at 0.5 L/min in the dark for 30 min to reach the adsorption equilibrium. After that, the sample was UV-irradiated for 180 min under otherwise identical conditions. Changes in acetaldehyde or toluene concentration were measured with a FID Shimadzu GC-14A gas chromatograph.

3. Results and Discussion

Effects of the Preparation Parameters on the Characteristics of the TiO_2 Films. For the preparation of transparent TiO_2 films, the amount of each chemical, as described in the Experimental Section, was optimized. In particular, the amount of HPC was essential. The surface area increased with increasing total amount of HPC. However, the films prepared with a too high amount of HPC became gradually white on increasing N and finally too opaque.

The optimal calcination temperature for preparing the TiO_2 films was decided from thermal analysis of the TiO_2 gel formed from the dip-coating solution. As shown in Figure 2, some peaks appeared at temperatures below 673 K. They could be due to the combustion of organic compounds. The sharp peak at 729 K may be attributed to the combustion of an organic gas initially trapped in the gel and released when the TiO_2 nanoparticles shrank and crystallized. Weight loss stopped around 753 K, meaning that all organic compounds were removed. Therefore, we selected 753 K as the appropriate calcination temperature for the preparation of the TiO_2 films.

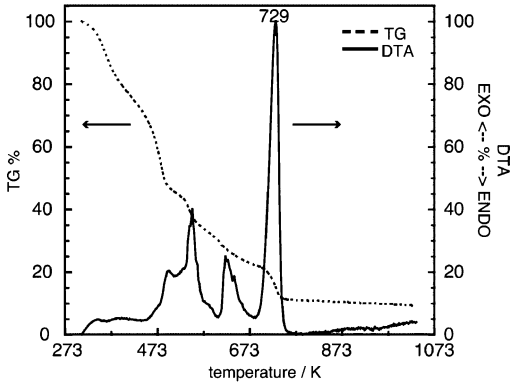

Figure 2. Thermal gravimetric (TG) and differential thermal analysis (DTA) curves for a TiO_2 gel.

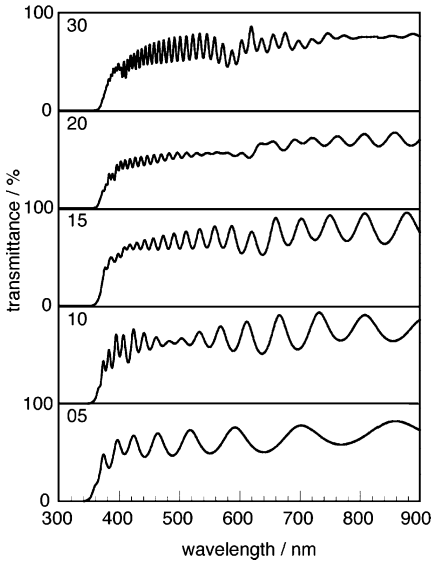

Figure 3. Transmission of TiO_2 films prepared with the number N ($5 \le N \le 30$) of dip-coating/calcination procedures indicated.

Table 1. Optical Properties, Thickness, and Contact Angle of the TiO_2 Films for the Number of Coatings *N* Indicated

	N				
	5	10	15	20	30
light transmitted through the TiO_2 layer in the visible spectral region (%)	66.0	71.0	73.0	64.0	69.0
light absorbed by the TiO_2 layer at 358 nm (%)	89.9	97.6	99.4	99.9	100.0
film thickness (μm) (optical method)	0.9	1.7	2.5	3.5	5.3
film thickness (μm) (SEM)	0.8	1.6	2.4	3.2	5.4
contact angle before UV irradiation (deg)	17.3	29.7	29.9	31.4	35.3
contact angle after a 2 h UV irradiation (deg)	7.4	6.3	6.7	7.2	6.9

The thermal treatment after dip-coating gave transparent TiO_2 films regardless of the film thickness for the optimal composition of the coating solution described in the Experimental Section. The average percentage of light transmitted through the TiO_2 films in the 500−900 nm (i.e., visible light) region was around 70%, regardless of N (Figure 3 and Table 1). This percentage takes into account both reflection and scattering: a glass plate without TiO_2 coating was used as the reference in the double-beam spectrometer. That may explain the slightly lower percentage for $N = 5$ because the

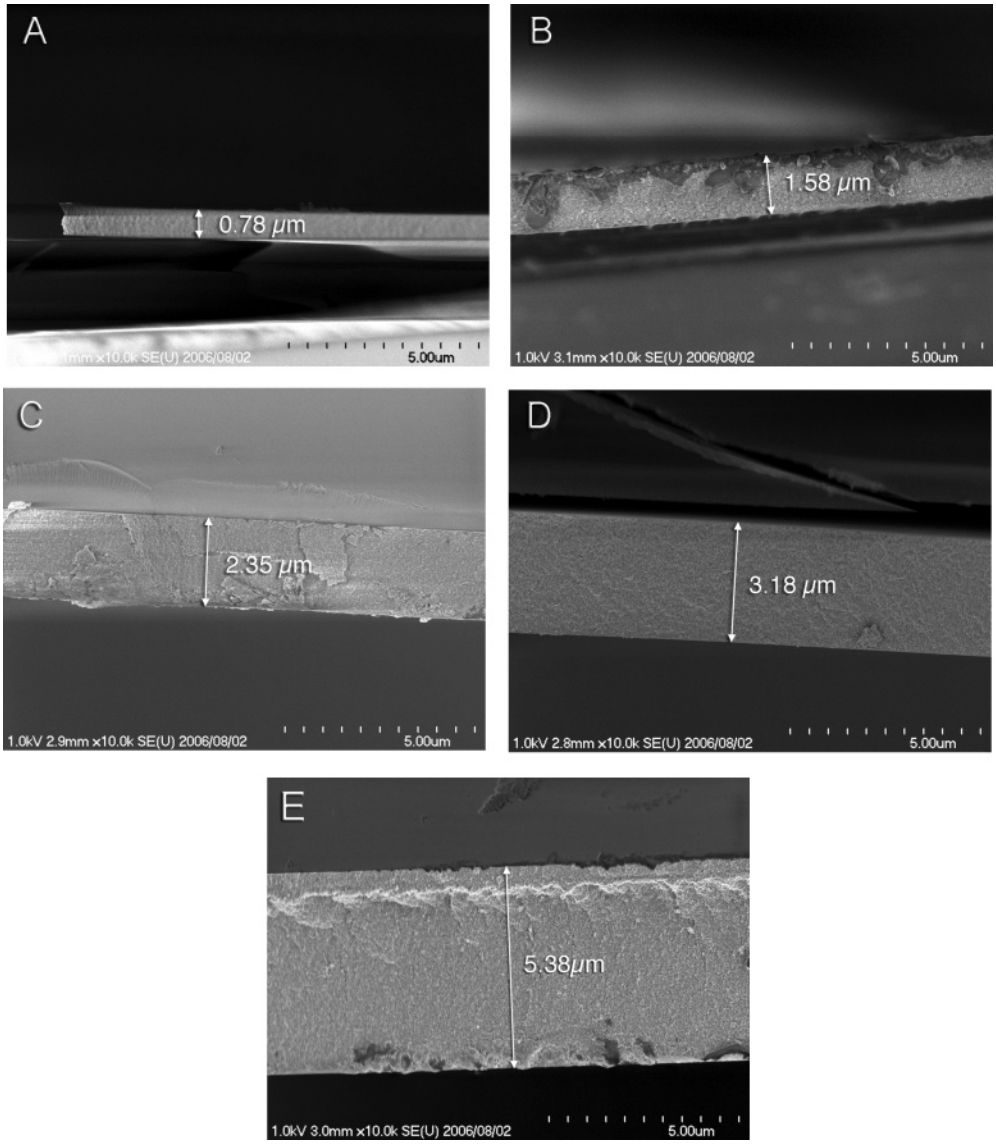

Figure 4. SEM images of the cross section of the TiO_2 films prepared with the following *N*: (A) 5, (B) 10, (C) 15, (D) 20, and (E) 30.

thinner the film, the higher the scattering of light. The waveform of the transmission spectra is caused by light interferences. The film thickness, *t*, can be calculated from the positions of the waveform peaks

$$t = \lambda_1\lambda_2/[2n(\lambda_2 - \lambda_1)] \quad (1)$$

where λ_1 and λ_2 are the wavelengths of adjacent pairs of minima and maxima, and *n* is the TiO_2 refractive index. For a TiO_2 crystal at room temperature, the value of *n* is 2.52; however, *n* decreases when the porosity increases.[35] We used 2.1.[15] The validity of this value was confirmed by the good agreement between the thicknesses thus calculated and those derived from SEM images (Figure 4 and Table 1).

Before UV irradiation, the contact angle of the water droplet on the surface increased with *N* (Table 1). After irradiation at 365 nm for 2 h with 1 mW/cm^2, the contact angle decreased to ca. 7° and, moreover, was not significantly affected by *N*. In this study, the purpose was not to investigate the self-cleaning and superhydrophilic properties of the TiO_2 films. However, these measurements of contact angle show that these properties exist, as expected.[8]

Panels A and B in Figure 5 show a linear relationship between *N* and the TiO_2 film thickness or weight. However, preparing thick films is time-consuming because of the repetitions of the dip-coating and calcination processes. Previously, we have reported that the increase in film thickness and weight with the use of HPC is higher than with that of polyethylene glycol (PEG); this difference was attributed to the higher viscosity of the HPC/TPO-containing dip-coating solution (ca. 14.6 cps against 11.5 cps for the PEG/TPO-containing dip-coating solution).[30]

The crystalline structure of the TiO_2 films was studied using XRD (Figure 6). The broad band at around $2\theta = 21°$ decreased with increasing *N*; consequently, it is thought to be due to the silica support of the TiO_2 films. The other XRD peaks are all attributed to anatase. The TiO_2 crystallite sizes, indicated in Figures 6 and 9, were calculated from the half width *b* of the XRD main peak at $2\theta = 25°$ using eq 2

$$r = K\lambda/(b\cos\theta) \quad (2)$$

(35) Yoldas, B. E.; Partlow, D. P. *Thin Solid Films* **1985**, *129*, 1.

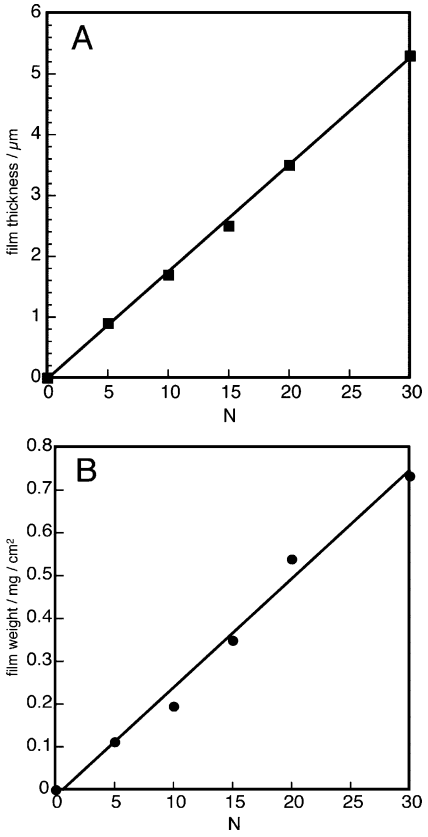

Figure 5. TiO_2 film thickness (A) and weight (B) against *N*.

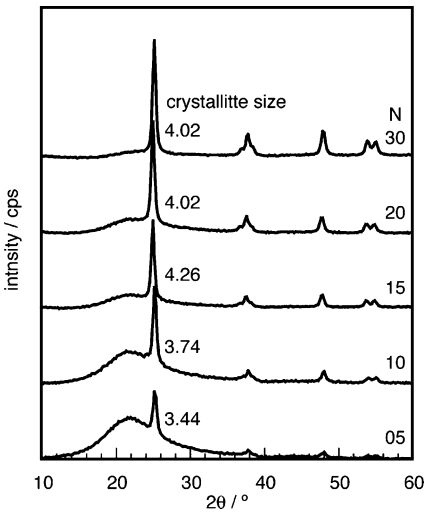

Figure 6. XRD patterns for TiO_2 films with the *N* indicated.

where λ is the wavelength of the X-ray.[15] We used $K = 1.38$, as reported by Kumar et al.[36]

Figure 7 shows that the surface area of the TiO_2 films decreased with increasing *N*. The pore size distribution slightly shifts toward larger values with *N* increasing from 5 to 10; however, no further shift was observed for higher *N* values (Figures 8 and 9). On the other hand, the pore volume decreased substantially with increasing *N* (Figure 9). The mean size of the TiO_2 crystallites calculated from the XRD main peak (Figures 6 and 9) was almost constant regardless of *N*.

(36) Kumar, K. P.; Keizer, K.; Burggraaf, A. J. *J. Mater. Chem.* **1993**, *3*, 1141.

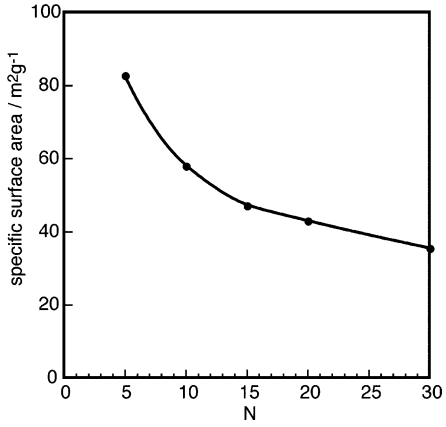

Figure 7. Surface area of TiO_2 films against *N*.

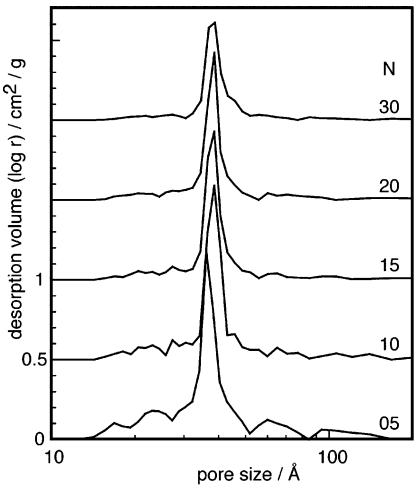

Figure 8. Pore size distribution of TiO_2 films against *N*.

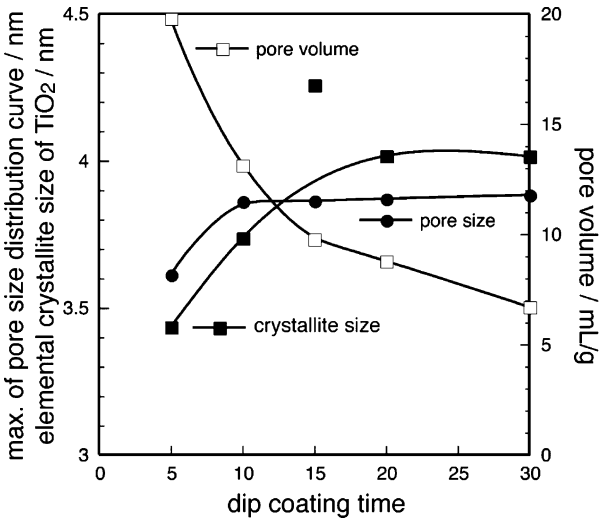

Figure 9. Size of anatase elemental crystallites, maximum of the pore size distribution curve, and pore volume of TiO_2 films against *N*.

AFM images (Figure 10) showed TiO_2 particles bigger than the crystallites whose size was calculated from XRD as shown in Figures 6 and 9, reflecting aggregation of crystallites upon calcination. The average size of the TiO_2 particles observed in Figure 10 in the film prepared with $N = 5$, 10, 15, 20, and 30 were 12, 17.9 (error was high because of the low resolution of the AFM image), 13.9, 15.7, and 16 nm, respectively. However, the difference of the surface structure between each films is quite little in an AFM image,

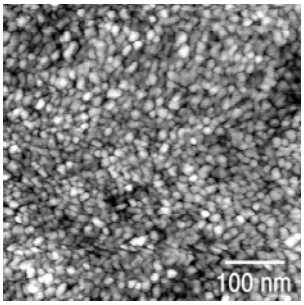

Figure 10. AFM images of TiO_2 film surfaces ($N = 30$).

and we showed alone the AFM image of $N = 30$. The absence of marked changes in particle size for $N > 15$ is in satisfactory accord with the lower changes in surface area (Figure 7) and pore size distribution (Figures 8 and 9) observed for $N > 15$.

Researchers[37−41] have used HPC to prepare TiO_2 coatings and reported that HPC molecules make cross-links between TiO_2 particles in the solution, which prevents agglomeration, so that tiny TiO_2 particles are obtained by subsequent calcination. However, the size of the TiO_2 crystallites prepared previously was still large (e.g., 12 nm after calcination at 773 K in the case of Gotic et al.)[37] compared with our samples. In our initial propan-2-ol solution, HPC formed a colloid with particles having a diameter of about 10 μm as measured with a laser particle size analyzer. We think the existence of this colloid explains why we obtained smaller particles. We infer that the formation mechanism of TiO_2 nanoparticles occurs as follows. When poured into the dip-coating solution, HPC form hydrogen bonds with TPOT.[41] It is assumed that TPOT molecules are thereby linked to the surface of the HPC colloids. Growth of TiO_2 crystallites from nuclei does not occur in the dip-coating solution, as formation of such nuclei is very likely hindered by HPC. To wit, the life time of the dip-coating solution is more than 1 year in an airtight vessel, that is, neither gelation nor precipitation take place. During the dip-coating process, HPC-bound TPOT sticks as a thick film to the SiO_2-coated glass because of the high viscosity. In this thick film, gelation does not occur except, perhaps, at the interface with humid air, and TiO_2 nanoparticles are formed only subsequently during calcination by TPOT transformation. Even during calcination, HPC and its decomposition products are thought to still limit aggregation of the elemental TiO_2 crystallites, so that the 12 nm particles shown by AFM images corresponded to the aggregation of only three 4 nm elemental TiO_2 crystallites (Figure 9).

The hardness of all films was greater than 9 H. In addition, the films did not peel off the silica-coated glass plates. Accordingly, it is expected that their durability is high enough for most uses. As, furthermore, they had an aforementioned transparency of ca. 70% in the 500−800 nm spectral region and did not whiten over time; they also meet the optical requirements for a number of applications.

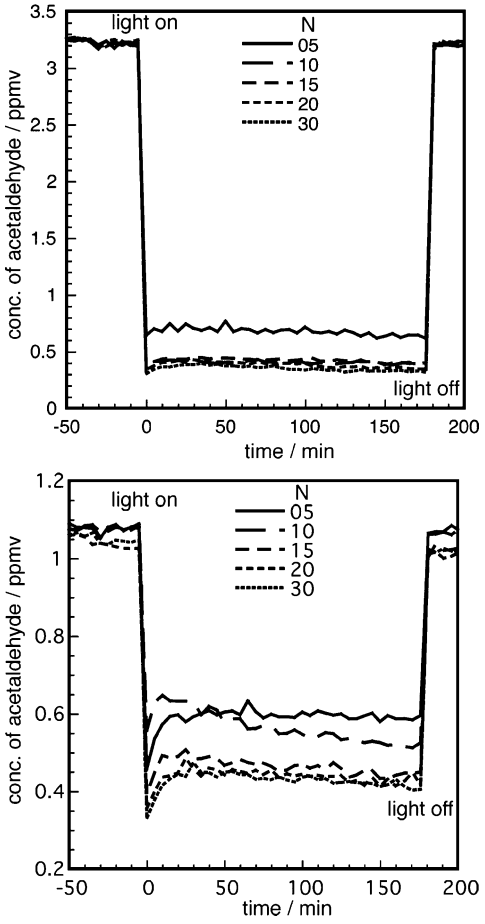

Figure 11. Kinetic variations in the concentration of acetaldehyde (A) and toluene (B) with or without UV irradiation for TiO_2 films with the N indicated.

Photocatalytic Activity of the TiO_2 Films. Figure 11A shows that concentration of acetaldehyde (ca. 3.25 ppmv) was drastically decreased under UV irradiation. As expected, this concentration immediately returned to its initial value after the irradiation was shut off. Under the experimental conditions used, the photocatalytic activity was lower for the film corresponding to $N = 5$ and nearly equal for the others (Figure 11A and Table 2). In the case of the removal of toluene (ca. 1 ppmv), the photocatalytic activity of the two thinner films was lower and those of the three thicker ones were almost equal (Figure 11B and Table 3). Switching off the UV irradiation made the toluene concentration regain its initial level.

The maximum removal rate was 5 times higher for acetaldehyde than for toluene (Tables 2 and 3). Assuming that the removal rate should be proportional to the concentration according to the Langmuir−Hinshelwood law for low concentrations, the ratio between the activities for acetaldehyde and toluene should be only about 3 times if the photocatalytic reactivities of both compounds were the same. Indeed, the photocatalytic removal rate of toluene has been reported to be lower than that of acetaldehyde,[42,43] as

(37) Gotic, M.; Ivanda, M.; Sekulic, A.; Music, S.; Popovic, S.; Turkovic, A.; Furic, K. *Mater. Lett.* **1996**, *28*, 225.
(38) Kim, K. D.; Kim, H. T. *Powder Technol.* **2001**, *119*, 164.
(39) Fang, C. S.; Chen, Y. W. *Mater. Chem. Phys.* **2003**, *78*, 739.
(40) Mohammadi, M. R.; Cordero-Cabrera, M. C.; Fray, D. J.; Ghorbani, M. *Sens. Actuators, B* **2006**, *120*, 86.
(41) Nagpal, V. J.; Davis, R. M.; Riffle, J. S. *Colloids Surf., A* **1994**, *87*, 25.
(42) Sano, T.; Negishi, N.; Takeuchi, K.; Matsuzawa, S. *Sol. Energy* **2004**, *77*, 543.
(43) Muggli, D. S.; Ding, L. *Appl. Catal., B* **2001**, *32*, 181.

Table 2. Photocatalytic Removal of Acetaldehyde Using Different TiO_2 Films

number of coatings *N*	film thickness (μm)	concentration of acetaldehyde (ppmv)	acetaldehyde amount removed (μmol/h)	acetaldehyde removed (%)	acetaldehyde removed calculated from absorption[a] (%)
5	0.9	3.25	3.39	80.3	80.8
10	1.7	3.24	3.78	87.7	87.7
15	2.4	3.24	3.71	88.0	89.4
20	3.5	3.26	3.78	89.1	89.8
30	5.3	3.25	3.80	89.9	89.9

[a] These percentages were calculated by multiplying the percentage for a 5.3 μm thickness (100% absorption at 358 nm) by the values of Table 1.

Table 3. Photocatalytic Removal of Toluene Using Different TiO_2 Films

number of coatings *N*	film thickness (μm)	concentration of toluene (ppmv)	toluene amount removed (μmol/h)	toluene removed (%)	toluene removed calculated from absorption[a] (%)
5	0.9	1.08	0.61	45.7	53.4
10	1.7	1.08	0.69	51.9	58.0
15	2.4	1.06	0.74	57.2	59.0
20	3.5	1.04	0.74	58.2	59.3
30	5.3	1.04	0.76	59.4	59.4

[a] These percentages were calculated by multiplying the percentage for a 5.3 μm thickness (100% absorption at 358 nm) by the values of Table 1.

expected, because the carbonyl group can be easily oxidized whatever the oxidizing method. Tables 2 and 3 show that the photocatalytic removal rate did not increase above a film thickness comprised between 0.9 and 1.7 μm or 1.7 and 2.4 μm for acetaldehyde or toluene, respectively, for differing concentrations but identical air flow rate, irradiance, and size of TiO_2-coated plate. Not surprisingly, a higher amount of UV-irradiated TiO_2 was needed for the less reactive compound in spite of a lower concentration. The preceding thickness values suggest that the irradiation penetration depth was higher than 1.7 μm and lower than 2.4 μm, in agreement with the percentage of light absorbed by the TiO_2 layer at 358 nm (Table 1), which is the wavelength of the lamp employed in the photocatalytic experiments. Indeed, the percentages of acetaldehyde removed calculated from the relative absorbance were very close to the percentages measured (Table 2). For toluene (Table 3), these percentages differed significantly for the two lowest thicknesses; in these latter cases, the lower percentages removed relative to those expected from the mere effect of the absorbance presumably reflect the difficulty for toluene to reach the most inner layers of UV-irradiated TiO_2 within the coating.

The lower percentage of toluene removed compared with acetaldehyde can not only be due to the aforementioned differences in (i) reactivity with respect to oxidation and (ii) reactant penetration depth into the coating but also to the competition between the initial pollutant and its degradation intermediate products for reacting with the photogenerated active species.[44] This competition should obviously be more pronounced for toluene, which possesses a higher number of C atoms and thus gives rise to a higher number of degradation intermediate products. In practice, to achieve complete removal under otherwise identical conditions, the size of the TiO_2-coated plate (Figure 1 B) should be increased more in the case of toluene.

Conclusion

To prepare micrometer-thick TiO_2 films on silica-coated glass plates, dip-coating/calcination stages were repeated. Our preparation strategy was based on the following features: (i) the increase in the viscosity of the dip-coating solution by use of α-terpineol; (ii) the introduction in the dip-coating solution of a hydroxypropyl cellulose that bound to tetraisopropyl orthotitanate (TPOT) and hence separate the TPOT molecules, rendering the dip-coating solution stable and thereby reusable; (iii) the transformation of TPOT into TiO_2 not by hydrolysis in the dip-coating solution as in the conventional sol−gel process but by calcination of the dip-coated layer; and (iv) the optimization of both the proportions of the dip-coating solution components and the calcination temperature. The TiO_2 layers thus obtained were hard, did not peel off the silica-coated glass plates, had a transparency of ca. 70% in the 500−800 nm spectral region even at a thickness of 5.4 μm, and did not whiten over time. Photocatalytic tests were also performed under representative outdoor conditions (value of UV-A irradiance; concentrations of two typical organic pollutants) to estimate the lowest layer thickness, and hence the smallest number of repetitions of dip-coating/calcination stages, necessary for achieving a near-maximum depollution of ambient air, at least in relatively confined spaces such as canyon streets.

Acknowledgment. N.N. gratefully acknowledges the France−Japan PICS joint research program, which allowed him to carry out experiments in Lyon.

CM070320I

(44) d'Hennezel, O.; Pichat, P.; Ollis, D. F. *J. Photochem. Photobiol., A* **1998**, *118*, 197.